*36th EPS Conference on Plasma Phys. Sofia, June 29 - July 3, 2009 ECA Vol.**33E**, P-2.143 (2009)*

Stability of Snowflake Diverted and Negative Triangularity Plasmas in the TCV Tokamak

S.Yu.Medvedev[1], A.A.Ivanov[1], A.A.Martynov[1], Yu.Yu.Poshekhonov[1], Y.R.Martin[2], J-M.Moret[2], F.Piras[2], A.Pitzschke[2], A.Pochelon[2], O.Sauter[2], L.Villard[2] and the TCV team.

[1]*Keldysh Institute, Russian Academy of Sciences, Moscow, Russia*
[2] *Ecole Polytechnique Fédérale de Lausanne (EPFL), Centre de Recherches en Physique des Plasmas, Association Euratom-Confédération Suisse, Lausanne, Switzerland*

The TCV experimental campaign aims at studying H-mode plasmas and ELM behavior in various diverted configurations including equilibria with negative triangularity [1] and snowflake divertor. Although the TCV tokamak is capable of generating plasma cross sections with a large variety of shapes, certain combinations are excluded by technical constraints. In particular, for diverted configurations, the strike points should be placed in regions covered by graphite tiles, which can support the local power densities.

A second order null divertor (snowflake) has been successfully created and controlled in the TCV tokamak [2]. Variations of the edge stability for the snowflake equilibria at different values of triangularity are investigated.

1 Stability of negative triangularity equilibria

The values of the $n = 0$ growth rates are very high for the negative (both upper and lower) triangularity equilibria in the TCV tokamak presented in [1] with a reference elongation $\kappa = 1.75$: $\sim 1500\,s^{-1}$. The growth rate is further increased when taking into account the ports (modeled as very high resistivity axisymmetric pieces of the wall): $\sim 3000\,s^{-1}$ in the reference plasma position and even can go ideally unstable when the plasma is shifted inside farther from the LFS wall. It confirms the conclusion about the high sensitivity of vertical stability for negative triangularity configurations to the distance between the outer wall and the plasma. A lower elongation is needed for negative triangularity configurations to be vertically controllable. Growth rates of axisymmetric modes were computed for fixed boundary equilibrium series with negative triangularity and elongation $\kappa = (\kappa_{up} + \kappa_{down})/2$ varied from 1.4 to 1.75. The up-down non-symmetric plasma boundary was prescribed keeping the ratio $\kappa_{up}/\kappa_{down} = 0.75$ and with triangularity $\delta_{up} = \delta_{down} = -0.65$. The dependence of the $n = 0$ growth rates is close to linear in $(\kappa - 1)$ and the growth rate value doubles when κ varied from 1.4 to 1.75. The elongation $\kappa = 1.4$ corresponds to a reasonable growth rate $\sim 700\,s^{-1}$ without ports (a factor of 2 larger with axisymmetric openings in the place of ports). The upward shifted (away from the LFS port) plasma is more vertically stable, however the issues related to the separatrix strike point positions at the LFS wall are to be solved in this case.

With an elongation increased up to $1.5 - 1.6$, the divertor strike points can be placed in full toroidal coverage zones with graphite tiles at the LFS wall. The SPIDER free boundary equilibrium code was used to compute series of equilibria using the control plasma shape with elongations $\kappa_{up} = 1.2, \kappa_{down} = 1.8; \delta_{down} = -0.65$ and varying δ_{up} to be matched by the $\psi/\psi_{sx} =$

0.995 surface. Additional control points were used to place the separatrix legs at the LFS tiles. For the resulting free-boundary equilibria the value of the elongation is about $\kappa = 1.6$, upper triangularity varies from 0.3 to -0.4 and lower triangularity of the $\psi/\psi_{sx} = 0.95$ surface is around -0.65 (Fig.2). The $n = 0$ growth rates are in the range of $400 - 700\,s^{-1}$ ($700 - 1000\,s^{-1}$ with 2D openings) with a minimum attained for zero upper triangularity (Fig.3a). The vertical growth rates of the negative triangularity equilibrium are rather sensitive to the plasma proximity to the LFS wall and the presence of the ports (Fig.3b).

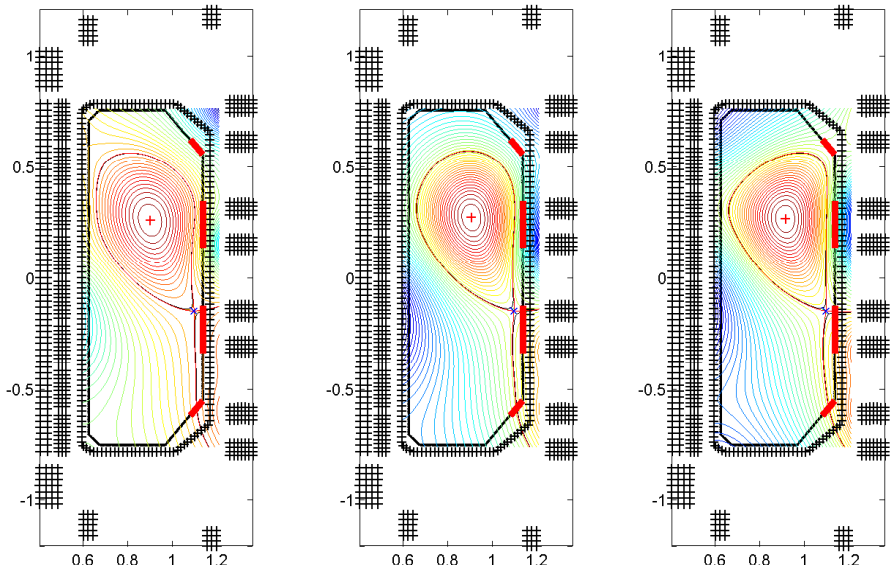

(a) (b) (c)

Figure 2. Poloidal flux level lines for free boundary equilibria in TCV tokamak calculated with the SPIDER code. Plasma elongation $\kappa \sim 1.6$. *Upper triangularities (a)* 0.3, *(b)* 0.0, *(c)* -0.4. *The positions of full toroidal coverage zones with graphite tiles are shown by thick red lines.*

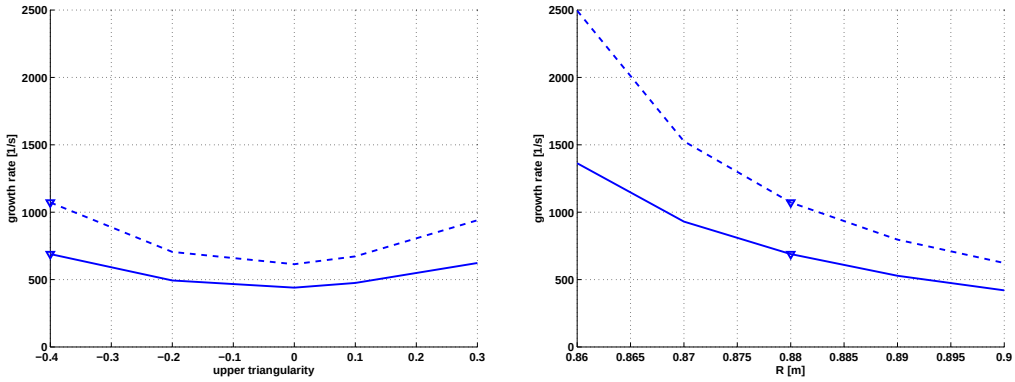

(a) (b)

Figure 3. Vertical instability growth rates for the TCV equilibria with elongation 1.6 *and negative lower triangularity versus (a) upper triangularity and (b) plasma center radius for upper triangularity* -0.4 *(Fig.2c, marked by triangles). Dashed lines correspond to the growth rates with 2D axisymmetric openings in place of ports in the TCV wall.*

The pedestal profiles from [3] and the plasma boundaries from Fig.2 a),b),c) were taken to generate the basic equilibria for edge kink/ballooning stability studies. The value of normalized current $I_N = 0.9$ was chosen to provide the safety factor on axis $q_0 \sim 1.1$. The stability diagrams

were obtained by the KINX stability code using equilibrium series with independently rescaled parallel current density and pressure gradient in the pedestal. The edge stability is mainly determined by the negative lower triangularity: the second stability access in the pedestal region is eliminated [1]. This can lead to different type of ELMs triggered by high-n ballooning modes at relatively low values of pressure gradient and current density in the pedestal. The low-n kink/ballooning modes $n = 1, 3$ were found more unstable with either positive or negative upper triangularity compared to zero upper triangularity case.

2 Equilibrium and stability of snowflake configurations

The free-boundary equilibrium code SPIDER (reconstruction mode) has been modified to compute equilibria with a snowflake divertor. An option to maintain the second order null in the prescribed position was added to the standard prescription of "limiter" points at the plasma boundary and a set of control points approximately specifying the target plasma shape while minimizing the sum of squared values of the coil currents. Let us note that it is sufficient to impose only two additional conditions, $\partial^2\psi/\partial Z^2 = 0$ and $\partial^2\psi/\partial R\partial Z = 0$, besides vanishing first derivatives at the second order null. Then the third one, $\partial^2\psi/\partial R^2 = 0$, is satisfied due to $\Delta^*\psi = 0$ for the poloidal flux function ψ in vacuum, where $\Delta^* = R(\partial/\partial R)(1/R)(\partial/\partial R) + \partial^2/\partial Z^2$ is the Grad-Shafranov operator. Using the reconstructed boundary for the TCV snowflake shot #36151 as a target shape, a variety of free boundary equilibria with different profiles and positions of the snowflake point has been obtained (Fig.4).

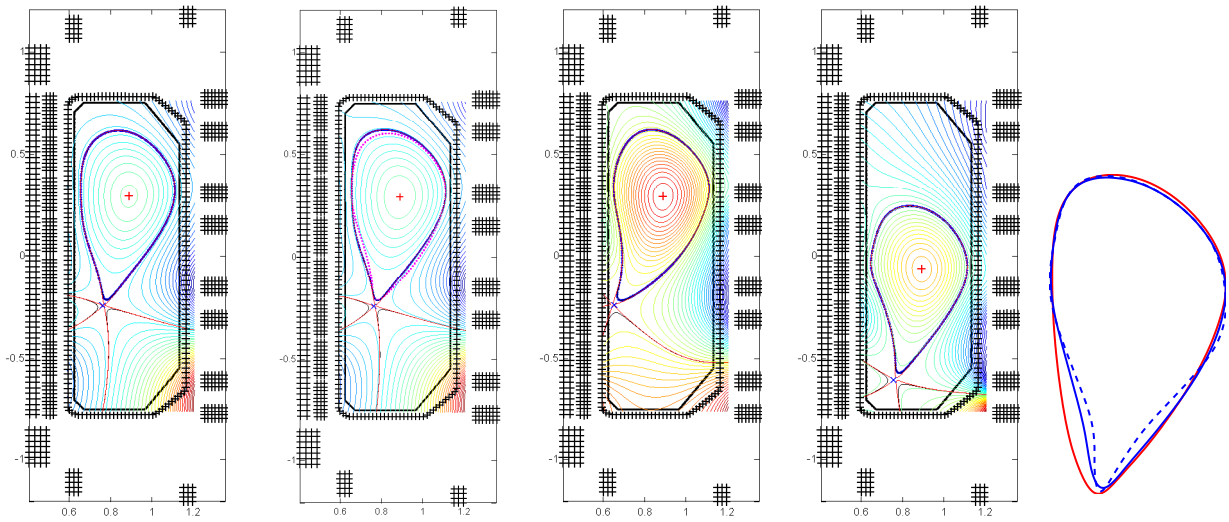

(a) (b) (c) (d) (e)

Figure 4. Poloidal flux level lines for free boundary snowflake equilibria: (a) fit to the shot #36151 boundary $\delta_{up} = 0.2$, (b) increased upper triangularity $\delta_{up} = 0.4$, (c) large snowflake point triangularity $\delta_{down} = 0.8$, (d) snowflake on the floor of the TCV vacuum vessel; (e) snowflake boundary from Fig.4b (blue) compared to the X-point boundary (red) and to the snowflake boundary with large pedestal current density (dashed).

The edge stability diagrams for the snowflake and standard X-point equilibria, also with the profiles from [3], are compared in Fig.5. The presence of the second order null leads to an

enhancement of the maximal attainable normalized pressure gradient $\alpha = 2\mu_0 dp/d\psi dV/d\psi \sqrt{V/(2\pi^2 R_0)}/(4\pi^2)$ especially in combination with the upper triangularity. Larger edge shear in the snowflake equilibrium results in a monotonic q profile maintained at larger values of the parallel current density $J_{||} = \max_{pedestal} < j \cdot B >$ (normalized by the cross-section averaged current density $< J >= I_p/S$) in the pedestal. However the current driven modes set the stability limit at approximately the same value of $J_{||}/ < J > \sim 1$ with the current driven mode $n = 1$ behaving much like $n = 3-5$ due to the higher density of rational surfaces $q = m/n$ in the pedestal region as a consequence of larger shear. Another feature of the free boundary snowflake equilibria is the significant sensitivity of the plasma shape in the vicinity of the snowflake point to the current density in the pedestal. In Fig.4e the plasma boundary for quadruple values of the pedestal current density and pressure gradient compared to the reference case is shown by the dashed line. The plasma boundary deformation leads to a further increase of the shear thus preventing its reversal even for very high values of pedestal current density. However, it does not give a significant edge stability limit enhancement.

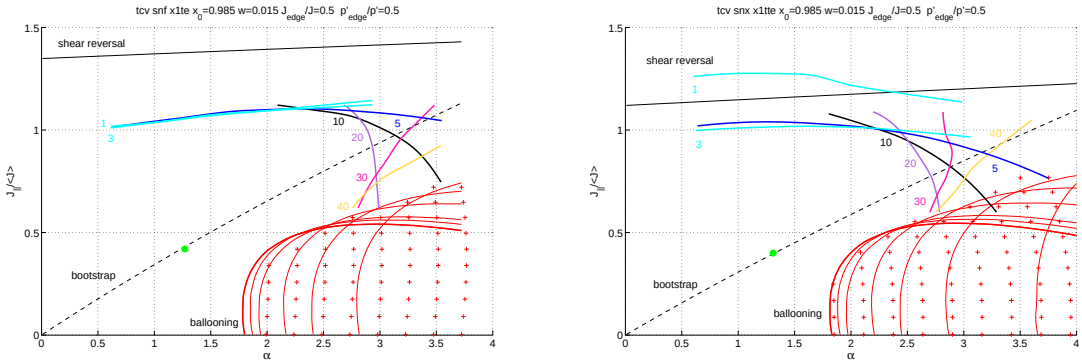

(a) (b)

Figure 5. Comparison of the edge stability diagrams for snowflake (a) and X-point (b) equilibrium (the shapes shown in blue and red in Fig.4e respectively). The crosses and red lines show the high-n ballooning mode stability boundaries. The shear is reversed above the solid black line. The dashed black line shows the collision-less bootstrap current density in the pedestal. Colored lines give the stability boundaries for medium $n = 5-40$ kink/ballooning modes (toroidal wave numbers are shown). Light blue lines show the stability boundaries for the global modes $n = 1,3$. The green circle corresponds to the pedestal parameters for the reference equilibrium.

As a conclusion, the edge stability of snowflake equilibria is enhanced compared to a standard X-point divertor plasma especially in a combination with increased upper triangularity: the values of the pedestal poloidal beta normalized by the pedestal width Δ (in the units of normalized poloidal flux [4]) that can be reached in the TCV snowflake configurations increases from $\beta_{\theta,ped}/\Delta$ = 4.5 to 5.5 ($\Delta = 0.06$ for the considered profiles). The value for ITER Scenario 2 is $\beta_{\theta,ped}/\Delta$=7-8.

[1] S.Yu.Medvedev *et al.* 35th EPS Conference on Plasma Phys. Hersonissos, 9 - 13 June 2008 ECA Vol.32D, P-1.072 (2008)
[2] F.Piras *et al.* Plasma Phys. Control. Fusion **51** (2009) 055009
[3] R.Behn *et al.* Plasma Phys. Control. Fusion **49** (2007) 1289
[4] P.B.Snyder *et al.* Physics of Plasmas **16** (2009) 056118

Acknowledgement *The CRPP authors are supported in part by the Swiss National Science Foundation.*